HHS Public Access

Author manuscript

Mucosal Immunol. Author manuscript; available in PMC 2020 November 04.

Published in final edited form as:

Mucosal Immunol. 2020 November ; 13(6): 908–918. doi:10.1038/s41385-020-0290-x.

Single cell and tissue-transcriptomic analysis of murine bladders reveals age- and TNFα–dependent but microbiota-independent tertiary lymphoid tissue formation

Marianne M. Ligon[1], **Caihong Wang**[1], **Erica N. DeJong**[2], **Christian Schulz**[2], **Dawn M. E. Bowdish**[2], **Indira U. Mysorekar**[1,3,*]

[1]Department of Obstetrics and Gynecology, Washington University School of Medicine, St. Louis, MO, 63110, USA.

[2]McMaster Immunology Research Centre, McMaster University, Hamilton, ON, Canada

[3]Department of Pathology and Immunology, Washington University School of Medicine, St. Louis, MO, 63110, USA.

Abstract

Aging has multifaceted effects on the immune system, but how aging affects tissue-specific immunity is not well-defined. Bladder diseases characterized by chronic inflammation are highly prevalent in older women, but mechanisms by which aging promotes these pathologies remain unknown. Tissue transcriptomics of unperturbed, young and aged bladders identified a highly altered immune landscape as a fundamental feature of the aging female bladder. Detailed mapping of immune cells using single cell RNA-sequencing revealed novel subsets of macrophages and dendritic cells and unique changes to the immune repertoire in the aged bladder. B and T cells are highly enriched in aged bladders and spontaneously form organized bladder tertiary lymphoid tissues (bTLTs). Naïve, activated, and germinal center B cells and IgA^+ plasma cells are found within bTLT and associated with increased urinary IgA concentrations. bTLTs form with increasing age and their formation is dependent on TNFα. Microbiota are not required to form bTLT form, as aged germfree mice harbor them. Thus, bTLTs require age-dependent TNFα but are independent of the microbiota. Our results indicate that chronic, age-associated inflammation underlies a fundamental alteration to the bladder and establishes a resource for further investigation of the bladder immune system in homeostasis, aging, and disease.

*To whom correspondence should be addressed: Indira U. Mysorekar, Ph.D., Washington University School of Medicine, Depts. of Obstetrics and Gynecology & Pathology and Immunology, 660 S. Euclid Ave., St. Louis, MO 63110, Phone: 314-747-1329, Fax: 314-747-1350, imysorekar@wustl.edu.

Author contributions

Conceptualization MML, CW, IUM. Methodology MML, CW, IUM, DMEB. Investigation MML, CW, CS, END. Data analysis MML. Resources IUM, DMEB. Supervision CW, DMEB, IUM. Funding IUM, DMEB. Visualization MML. Writing--original draft MML, IUM. Writing--review & editing MML, CW, DMEB, IUM

Competing Interests

The authors have no financial interests to disclose.

Data and materials availability

All sequencing data will be deposited in an appropriate public repository.

One Sentence Summary:

Mice develop bladder tertiary lymphoid tissue (bTLT) during aging that is dependent on TNFα

Keywords

single cell RNA-sequencing; inflamm-aging; mucosal aging; lower urinary tract symptoms (LUTS); bladder disease; elderly

INTRODUCTION

Immune dysfunction during aging is characterized by chronic, low-grade inflammation, termed inflamm-aging[1]. Aging is the strongest risk-factor for many chronic diseases, including cardiovascular disease, neurodegeneration, osteoarthritis, and cancers[2]. While these diseases are all linked by chronic inflammation, immune responses vary by tissue, resulting in tissue-specific immune dysfunction[3].

The bladder is a storage organ with a mucosal barrier that provides protection from both urinary wastes and pathogens[4, 5]. Bladder diseases are highly prevalent among the elderly, and women are predominately affected by these diseases[6–9]. Older women (50+) are highly susceptible to bladder disorders including overactive bladder/urge incontinence (OAB), interstitial cystitis/bladder pain syndrome (IC/BPS), and recurrent urinary tract infections (rUTIs). These disorders all have a chronic inflammatory component as well as overlapping symptoms, known as lower urinary tract symptoms (LUTS)[10–12]. How and why these bladder diseases become more prevalent with aging is not currently understood[9]. Given the common association of bladder diseases with both aging and chronic inflammation, local immune dysfunction at the bladder mucosa may underlie mechanisms driving age-related bladder diseases.

During homeostasis, bladder immune cells consist of ~80% antigen-presenting macrophages and dendritic cells, ~10% T cells, and small numbers of NK cells, mast cells, eosinophils, and patrolling monocytes[13, 14]. Whether aging affects immunity in the bladder mucosa is not known; however, since chronic bladder inflammation is highly prevalent in older women, age-associated disruption of immune homeostasis in the bladder may mediate inflammatory pathology and lower urinary tract symptoms.

The bladder lacks dedicated mucosal secondary lymphoid organs (SLOs) that form during development like the Peyer’s patches of the small intestine, resulting in a uniquely quiescent bladder mucosal immune system. Non-lymphoid organs may sometimes form ectopic, SLO-like structures in response to chronic inflammation and antigen exposure[15–17]. Lymphoid aggregates have been reported in cases of chronic bacteriuria, muscle-invasive bladder cancer, and IC/BPS[18–20]. However, lymphoid aggregates in the bladder remain largely uncharacterized and are not reported to spontaneously form in the mouse bladder. Furthermore, factors influencing their formation, composition, or persistence, have not been identified.

In this report, we sought to identify underlying effects of aging on bladder tissue and the bladder immune cell repertoire using global tissue transcriptomics and targeted, single-cell transcriptomics from young and aged mouse bladders. We find that aging fundamentally alters the bladder immune landscape on the cellular and tissue-transcriptomic levels. We demonstrate that in unperturbed aged bladders, expanded numbers of B and T cells organize into structures we term bladder tertiary lymphoid tissue (bTLT). bTLT in aged mice serve as centers for B cell recruitment, activation, and differentiation into plasma cells. Age-dependent bTLT form in aged germ-free mice, but aged TNFα$^{-/-}$ mice have fewer and smaller bTLT, indicating that bTLT require age-dependent TNFα but are independent of the microbiota. Together these data reveal a profound change in the bladder mucosal immune system that is fundamental to aging in this tissue.

RESULTS

Tissue and single cell transcriptomics reveal substantial effects of aging on the bladder immune system

Older age is associated with many bladder diseases, yet little is known about the fundamental changes to the bladder that occur during aging. Since women have a higher prevalence of bladder disorders and have distinct lower urinary tract anatomy, physiology, and age-related changes from men[21], we chose to study how aging affects the bladder using aged female mice as a model. We first sought to characterize age-related global transcriptomic changes to the bladder by performing RNA-sequencing (RNA-seq) on whole bladder tissue from young (3 month old) and aged (18 month old) female mice. Bladders from aged mice had at least a 2-fold increase in expression of 416 genes and decrease in expression of 60 genes compared to those from young mice (Fig. 1A, Benjamini-Hochberg adjusted false discovery rate (FDR) ≤0.05, Supplementary Table 1). We then performed pathway analysis of all expressed genes using the Kyoto Encyclopedia of Genes and Genomes (KEGG) pathway database and identified 13 up-regulated pathways and 1 down-regulated pathway in the bladder transcriptome of aged mice compared to those of young mice (Fig. 1B). Highly up-regulated pathways included antigen presentation, B- and T-cell activation, cytokine-receptor interactions, and intestinal IgA production (Fig. 1B–C). Enrichment of these pathways suggested that immune cells may be recruited to and activated within the aging bladder. Using independent samples, we validated increased expression of the most highly upregulated chemokine, *Cxcl13* (Fig. 1D), a homeostatic lymphoid chemokine that attracts naive lymphocytes to organized lymphoid tissues. We examined expression of the 3 other homeostatic lymphoid chemokines, finding that *Ccl19*, but not *Cxcl12 or Ccl21*, was also upregulated in aged bladders (Fig. 1D, Fig. S1). In mice, bladder tissue typically harbors a small number of immune cells compared to other mucosal barriers, and many of these cells have unknown functions in bladder homeostasis or disease[4, 13, 22]. Using flow cytometry, we found that aged bladders contained nearly 3 times as many CD45^{+} cells as young bladders (Fig. 1E), further indicating that the tissue transcriptomic changes we observed were likely due to high numbers of immune cells in aged bladders compared to young bladders. Notably, *Tnf* was also among the most highly upregulated cytokines in the aged bladder (Fig. 1C). TNFα plays a role in driving inflamm-aging and is a predictor of frailty and mortality in humans[23, 24]. Along with chemokine-mediated recruitment, locally

increased TNFα in the bladder could be driving an age-associated inflammatory environment and activating immune cells in the aged bladder. Since the bladder mucosa is normally immunologically quiescent, these data suggested that an altered immune landscape was fundamental to the aging bladder.

To take an unbiased approach to identifying the immune cell types that were driving the immune cell accumulation and tissue transcriptomic changes in aged bladders, we performed droplet-based single-cell RNA-seq (scRNA-seq) on enriched $CD45^+$ cells isolated from young and aged bladders. After removing urothelial and stromal cells from analysis, we identified 21 distinct immune cell clusters (Fig. 2A, Fig. S2–3). Using canonical cell type markers and queries against the ImmGen database of immune cell transcriptomes[25, 26], we assigned identities to all of the immune cell clusters (Table 1, Supplementary Tables 2–3). We identified immune cells that have been previously reported in bladder tissue, including macrophages, monocytes, dendritic cells (DCs), natural killer cells, γδT cells, and both $CD4^+$ and $CD8^+$ αβT cells[13, 14, 27, 28]. In both young and aged bladders, we identified 2 distinct macrophage clusters distinguished by high expression of *Retnla* in the smaller cluster (Fig. S4A). *Retnla* (also known as Relmα or *Fizz1*) is a marker of alternatively activated macrophages; thus, this macrophage cluster may have a more pronounced tissue-reparative phenotype compared to the larger macrophage cluster. Interestingly, a small, third cluster of macrophages were exclusively found in the aged bladder (Fig. 2B, Fig. S4B) and were distinguished by high expression of *Cxcl13* (Fig. 2C), one of the most highly upregulated genes identified by tissue RNA-seq. While there were not surface markers to distinguish these cells, we were able to detect highly increased expression of *Cxcl13* in sorted $F4/80^+CD64^+Ly6C^-$ macrophages from aged mice compared to those from young mice (Fig. 2D). Thus, macrophages are the most likely source of the high *Cxcl13* expression identified in the tissue transcriptome of the aged bladder and likely contribute to immune cell recruitment during aging. We also identified a distinct cluster of type 1 classical DCs (cDC1), which most likely correlate to previously reported $CD103^+$ DCs, and 3 clusters of type 2 cDC (cDC2), likely corresponding with previously reported $CD11b^+$ DCs[13, 29]. However, we were unable to detect mast cells, which are known to play important roles in bladder inflammation and infection, or eosinophils, which have also been previously reported within mouse bladder tissue[13, 29, 30]. These cells may not have been isolated by our methods or the populations may too small to resolve by clustering since they are known to be minor immune cell populations within the bladder. Our transcriptional analysis of the bladder immune repertoire at single-cell resolution is generally consistent with the literature while also identifying novel subsets of cells that may play distinct roles in bladder homeostasis, aging, and disease.

The most striking difference in the immune cell repertoire between young and aged bladders was a dramatic increase in B and T cells within aged bladders (Fig. 2B, Fig. S4B). B cells are generally absent from young bladders, and T cells comprise only a small number of cells in young bladders[13]. The largest cluster of B cells were naive B cells marked by strong *Ighd* expression (Fig. S3, Fig. S4C). Two smaller B cell clusters expressed markers of activated B cells, such as *Ctla4* and *Mzb1* (Fig. S4C). In one B cell cluster, 95% of cells expressed a specific immunoglobulin germ-line variable genes (Fig. S3, Fig. S4C, Supplementary Table 2), suggesting that some of these B cells may have been clonally expanded. Both B cell

clusters also expressed *Fcrl5* (Fig. S4C), a marker of dysfunctional B cells, termed age-associated B cells (ABCs), which have been implicated in inflamm-aging and autoimmune disorders. The exact function of ABCs is debated due to their similarity to a subset of atypical memory B cells[31,32]. scRNA-seq also demonstrated an increase in plasma cells in aged bladders. Plasma cells expressed high levels of *Jchain* (Fig. S4C), which forms part of the multimeric, secretory forms of IgM and IgA. Thus, a spectrum of B cell states, including naive, activated, and differentiated B cells, were present in the aged bladder and could potentially be participating in active, local immune responses.

Lymphocytes in aged mouse bladders organize into tertiary lymphoid tissues

Since aging resulted in a substantial increase of lymphoid cells in the bladder according to scRNA-seq analysis, and little is known about these cell types in the bladder, we further investigated these cells in aged bladders. Flow cytometry confirmed that aged bladders indeed harbored a significant increase in total T cells, $CD4^+$ and $CD8^+$ T cell subsets, and B cells compared to young bladders (Fig. 3A). To investigate how the influx of lymphocytes affected the bladder tissue architecture, we examined bladders histologically. Surprisingly, we found that the majority of aged bladders contained large aggregates of lymphocytes in the lamina propria that were completely absent in young bladders (Fig. 3B). Since aging is a continuous and highly variable process, we examined bladders from mice aged 3 to 18 months (m) (Fig. 3C). We found that lymphoid aggregates first appeared in some bladders at 9 m, and all bladders contained these structures at 15 m. These observations indicated that lymphoid aggregates began to form in ‘middle’ age and became a common feature of mouse bladders by 18 m (approximately equivalent to 60 years old in humans). These structures led us to hypothesize that the B and T cells accumulating in the bladder during aging were accumulating within these aggregates. Indeed, bladder lymphoid aggregates in aged mice were primarily composed of $CD3^+$ T and $B220^+$ B cells, while these cells were not found elsewhere in the lamina propria (Fig. 3D). In larger aggregates, B and T cells tended to segregate into respective zones, reminiscent of the highly organized structure of lymphoid tissues, such as lymph nodes[15, 16]. Lymphoid tissues contain specialized structures that facilitate their form and function in generating B cell responses. In the aged bladder, we identified $CD31^+$ (platelet endothelial cell adhesion molecule, PECAM) vessels that also expressed peripheral node addressin (PNAd), a specific marker of specialized, high endothelial venules (HEVs) (Fig. 3E). HEVs are otherwise only found in lymphoid tissues and facilitate the circulation of naive lymphocytes into the structure. We also found $CD35^{hi}$ (complement receptor 1, CR1) follicular dendritic cell (FDC) networks within larger aggregates (Fig. 3F). FDCs are stromal cells that structurally support the organization of lymphoid tissues. These findings demonstrate that aged bladders, but not young bladders, contain lymphoid aggregates with features of organized lymphoid tissue; thus, hereafter we term these structures bladder tertiary lymphoid tissues (bTLTs). TLTs typically elaborate functions that otherwise only occur within the secondary lymphoid organs, but TLTs are localized to the site of inflammation and immune response[15, 16]. Lymphoid aggregates have been reported in a few models of chronic bacteriuria and bladder cancer but remain poorly characterized and have thus far not been reported in unperturbed bladders[18, 19, 33]. Since bTLTs are specifically found in aged bladders, they could facilitate inflamm-aging within the bladder tissue and significantly alter immune responses to a variety of stimuli. To begin

to understand these structures, we sought to further characterize them and determine their functional capacity during aging.

bTLTs contain germinal centers and promote class-switched IgA responses

Since our scRNA-seq data indicated the presence of a range of B cell states, we hypothesized that there were active B cell responses occurring within bTLTs. Like their SLO counterparts, TLTs can support germinal center (GC) reactions where B cells are activated by antigen recognition, may undergo further selection, affinity maturation, and class-switch recombination, and differentiate into plasma cells that secrete large quantities of antibodies[34, 35]. We found that a large number of B cells in bTLTs were IgD^+ naive B cells (Fig. 4A), consistent with our scRNA-seq data. Locally active GCs were identified within bTLTs by the highly-specific GC marker GL-7 (Fig. 4B). We confirmed the presence of increased numbers of $CD138^+$ (Syndecan-1^+) plasma cells by flow cytometry (Fig. 4C) and localized them to bTLT (Fig. 4D), indicating that differentiated B cells were also part of these structures. While the majority of plasma cells identified by scRNA-seq expressed *Ighm* (Fig. S2C), the presence of GCs within bTLTs suggested that class switch recombination (CSR) may occur locally. Furthermore, we demonstrated that larger bTLTs contained GCs where CSR typically takes place. Tissue RNA-seq also indicated that multiple class-switched isotypes were enriched within the aged bladder (Fig. 4E). The most highly enriched, class-switched isotype was IgA, which is the major secretory isotype. This finding agreed with the enriched intestinal IgA production pathway we previously identified in aged bladders (Fig. 1B), which includes processes that typically occur at Peyer's patches in the intestinal mucosa. IgA is found in urine and polymeric Ig receptor (pIgR), which transports secretory IgA across epithelial barriers, is expressed in the urothelium[36, 37]. However, little is known about the local production, transport, and regulation of IgA at the bladder mucosa. To determine if increased IgA was locally produced in the aging bladder, we first measured IgA concentration in the urine. Urine from aged mice contained ~10-fold higher concentrations of IgA compared to urine from young mice (Fig 4F). In the kidney, IgA transport by pIgR is decreased during aging, which may contribute to IgA deposition at the glomerulus[38]. *Pigr* was not identified as significantly up- or down-regulated in our tissue RNA-seq data, and independent quantification of *Pigr* expression in bladders from young and aged mice did not show any significant differences (Fig. S5). These data suggest the increased urine IgA in aged mice is likely due to increased local production and not changes in the excretion rate of IgA. To further determine if the increased amount of IgA was locally produced, we cultured bladders *ex vivo* for 24 hours, finding that aged bladders consistently produced higher concentrations of IgA than young bladders (Fig. 4G). Furthermore, we identified IgA^+CD138^+ plasma cells associated with bTLT in aged bladders (Fig. 4B, D), indicating that these cells were locally differentiated and likely contributed to the high amounts of IgA in the urine from aged mice. Altogether, these findings indicate that bTLT in aged mice are functionally active in the local recruitment, activation, and differentiation of B cells into IgA-secreting plasma cells.

Age-associated bTLT form independently of microbiota but require TNFα

Both intrinsic and extrinsic factors influence age-associated changes in the immune system. Several lines of evidence point to the importance of microbial stimuli in TLT formation in

other tissues mucosal tissues including the lung and intestine[39, 40]. Furthermore, the intestinal microbiota significant changes in old age and correlates with markers of inflamm-aging[41]. To determine if microbes triggered age-associated bTLT formation, we examined bladders from aged germ free (GF) mice and age-matched, specific pathogen free (SPF) mice. Surprisingly, there were no differences in the number or size of bTLT in aged GF mice compared to SPF controls (Fig. 5A–B), demonstrating that a living microbiota is not required for age-associated TLT formation in the bladder. Tissue RNA-seq of young and aged bladders identified a number of cytokine and chemokine mediators that are likely involved in age-associated bTLT formation (Fig. 1C). In particular, we identified and validated increased expression of *Tnf* (TNFα, Fig. 5C), a pro-inflammatory cytokine that increases during aging and impacts age-related pathologies[23, 24, 39]. While TNFα is required during acute immune responses, particularly to combat bacterial infection, excess or prolonged TNFα can lead to disease. The role of age-associated TNFα in many tissues, including the bladder, remain unknown. To test whether increased TNF with age was a key driver of bTLT formation, we aged TNFα$^{-/-}$ mice to 18–24 m and examined their bladders for bTLT formation. While aged TNFα$^{-/-}$ mice had small, perivascular infiltrates in the bladder (Fig 5B), they had fewer and smaller bTLT than age-matched WT controls (Fig. 5C). Due to the rarity of bTLT in aged TNFα$^{-/-}$ mice, we were unable to identify comparable structures by immunofluorescence. These data suggest that age-associated TNFα plays a significant role in the expansion and/or maturation of bTLT but may not be responsible for the initial recruitment of small numbers of lymphocytes to the aging bladder. In the context of our overall findings, age-associated TNFα is an important mediator reshaping the immune landscape in the aging bladder to promote the formation of bTLTs.

DISCUSSION

The consequences of immune aging on mucosal tissues such as the bladder are only beginning to be unraveled[21]. To gain insight into the connection between aging, inflammation, and bladder disease, we sought to define how aging affects the bladder in an unperturbed state. At the tissue transcriptomic level, we found that nearly all highly significant changes point to an altered immune landscape being a fundamental feature of the aging bladder. The presence of lymphoid aggregates, composed of B and T cells organized into bladder tertiary lymphoid tissue (bTLT), underlie these tissue-level transcriptomic changes. Our findings suggest that age-associated inflammation, or inflamm-aging, could explain why aging is a risk factor for a plethora of bladder diseases. Bladder diseases are highly prevalent among women over 55 and continue to increase with age[9, 21]. For example, overactive bladder (OAB) affects approximately 50% of women over age 65[6]. Inflamm-aging is proposed as a causative or exacerbating factor of OAB, and one study found that elevated urinary CCL2, CXCL1, and nerve growth factor (NGF) correlated with age in OAB patients[12]. Women over age 55 are also more susceptible to recurrent urinary tract infections (rUTIs)[8]. Mouse models of rUTIs have demonstrated that a history of chronic bacteriuria, characterized by severe inflammation, predisposes to a more severe secondary infection after antibiotic treatment[42]. Interestingly, these mice develop lymphoid aggregates in the bladder, while those that resolve their infections do not[18]. The composition and structure of these aggregates have not been described; thus, it is unknown whether they are similar to bTLT

found in aged mice. Since aged mice harbor bTLT at steady state, the impact of these structures on the bladder tissue environment could be similar in these models. Our findings suggest that an altered or dysfunctional local immune repertoire in the aging bladder could explain why aging is a risk factor for multiple distinct bladder diseases. Considering the high prevalence of bladder diseases, an expanding aged population, and the relative lack of data on how established disease models differ with age, investigation of these bladder diseases in aged animals is warranted. Our work provides a framework establishing how the bladder differs between young and aged female mice at steady state, including the presence of bTLTs.

We also generated a single-cell resolution, transcriptomic map of resident immune cells within bladder tissue of both young and aged mice, identifying a plethora of immune cells and novel subsets. Prior single-cell studies have used the whole dissociated bladder, resulting in sparse immune cell analysis in this tissue[43–45]. In aggregate, these studies have identified macrophages, NK cells, 2 sets of dendritic cells, T cells, and monocytes. Using scRNA-seq of enriched immune cell populations, we identified known bladder immune cell populations as well as novel sets of immune cells. In the myeloid lineage, we identified 2 distinct subsets of macrophages, 4 subsets of classical DCs, monocytes, plasmacytoid DCs, and migratory DCs from both young and aged mice in our study. Bladder macrophage subsets could be distinguished by expression of *Retnla* (also known as RELMα or *Fizz1)*, a hallmark gene of an alternatively-activated macrophage (M2) phenotype. Macrophages typically play a role in tissue repair and homeostasis, but this function has not yet been investigated in the bladder. In aging, macrophages and other immune cells maintain tissue homeostasis by clearing debris as cells die, become senescent, or accumulate damaged proteins[46]. Impaired clearance of these cells by macrophages contributes to age-related pathologies and inflammation; in the aged bladder, failure to clear these cells could potentially lead to bTLT formation in an effort to compensate for this deficiency. We also identified a small group of macrophages expressing *Cxcl13* exclusively in the aged bladder. Since CXCL13 is a homeostatic lymphoid chemokine that attracts and organizes lymphocytes into SLOs and TLTs, these aged bladder macrophages likely play a key role in bTLT formation. While stromal cells are frequently a source of CXCL13 in other tissues, macrophages appear to take on this role in the aged bladder, demonstrating how the bladder may be a uniquely permissive tissue for TLT formation. In the lymphoid lineage, we identified B cells, NK cells, γδT cells, $CD4^+$ and $CD8^+$ T cells, and ILC2. The most striking difference between young and aged bladders was the largely expanded T and B cell compartments that made up the bTLT described herein. In whole, these data demonstrate that the bladder immune system is likely much more complex than previously appreciated and dramatically altered during aging. This single-cell transcriptomic map of bladder immune cells will be a resource to further dissect the function of different immune cells in bladder health, disease, and aging.

bTLT in the aging bladder represents an unexpected and significant shift of the immune repertoire in the steady state bladder. Unlike other mucosae, the bladder does not normally harbor organized lymphoid tissue; the finding is otherwise only reported in diseased bladder tissue. Here we determined the cellular composition and structural organization of age-associated bTLT and demonstrate that they contain active germinal center (GC) reactions. A

spectrum of B cell states was identified by scRNA-seq in aged bladders, including naive, activated, and atypical/dysfunctional memory B cells (or age-associated B cells), as well as a substantial increase in the number of antibody-producing plasma cells. B cell hematopoiesis is reduced in aging and results in oligoclonal expansion of existing B cells[47]. In humans, these observations derive primarily from peripheral blood, and in mice, most studies focus on the spleen and bone marrow. Here we show that B cells, including a large population of naive B cells, accumulate within the bladder tissue. B cell accumulation in tissues such as the bladder could be one factor contributing to the decline of B cells in the periphery. Our data showed that in aged mouse bladders, bTLT were capable of recruiting naive B cells to undergo local activation, GC reactions, and plasma cell differentiation.

TLT are more likely to form in aged tissues in response to stimuli. For example, in the lung, aged mice more robustly form inducible bronchus-associated lymphoid tissue (iBALT) in response to cigarette smoke exposure[48]. Aged mice also spontaneously develop distinct lymphocytic infiltrates in the lung, though these structures have not been formally defined to be iBALT[39]. In contrast to our findings in the bladder, age-associated lung infiltrates are greatly reduced in aged GF mice, highlighting tissue-specific differences in potential triggers of TLT formation. In the intestine, isolated lymphoid follicles (ILFs) develop after birth and thus are considered TLTs. A greater number of both mature and immature ILFs are found in aged mice compared to young mice, and these ILFs contain altered cellular compositions[49]. Interestingly, ILFs from aged mice produce lower amounts of chemokines yet produce more IgA than their younger counter parts. ILFs and their precursors are present in GF mice[50], but microbial colonization promotes the maturation of these TLTs[40], and intestinal microbiota are frequently the antigenic target of IgA produced therein[51]. These studies establish that TLTs do not absolutely require a live microbiota, implying that they could target non-microbial antigens as well. GF mice are still exposed to environmental, dietary, and altered-self antigens that could drive the formation and maturation of these structures. In the urinary tract, microbial colonization also does not appear to be required to form age-associated bTLT, suggesting that in the urinary tract environment, these TLT typically target non-microbial antigens. One explanation may be an increased burden of altered proteins in the urinary environment, which is designed to store these toxic wastes. TLTs have also been found in the liver and kidneys of aged mice, and drivers of these TLTs also remain elusive[52, 53].

Urine from aged mice had higher levels of IgA, and aged bladders supported increased local IgA production. In humans, IgA is elevated in the serum during aging[54, 55], and one study found IgA enriched in the urine proteome of elderly humans compared to young and middle-aged humans[56]. While total IgA appears to be elevated in both mice and humans, generation of antigen-specific IgA is impaired[57]. How IgA functions in the urinary tract remains ill-defined. IgA is increased during UTIs, particularly pyelonephritis, but whether it is protective in subsequent infections or dysregulated in those with rUTIs has not been shown[58]. Patients with selective IgA-deficiency are not reported to be more susceptible to UTIs, but this association has not been studied extensively and could be due to redundant or compensatory IgM[37]. The target antigens of homeostatic or bTLT-derived IgA in the urinary tract is unknown, and could be a response to cumulative UTIs over the life, age-associated antigens, tissue damage from long-term urine exposure, the urinary microbiome, or age-

associated dysfunctional B cell responses. Our data demonstrate that GF mice form similar numbers and sized bTLT, suggesting that non-microbial factors are likely causative. Further investigation of upstream factors influencing bTLT formation during aging and other urinary tract insults could begin to answer some of these questions.

We also identified a key, age-associated inflammatory cytokine, TNFα, as a mediator of bTLT formation in the aging bladder. Aged TNFα-deficient mice had reduced numbers and size of lymphoid aggregates compared to aged WT mice. TNFα is a mediator of inflamm-aging and has many roles in pathologic changes that arise during old age[23, 24]. Increased TNFα in centenarians is an independent risk factor for all-cause mortality, and chronic TNFα exposure impairs beneficial responses to pneumococcal pneumonia[23, 39]. However, TNFα is also essential for defense against pathogens, particularly extracellular bacteria. Indeed, TNFα is required for effective immune responses during UTIs[14, 59]. However, excess, inappropriate, or prolonged TNFα can promote pathologic changes leading to inflammatory disease and dysfunction during aging. TNFα contributes to interstitial cystitis/bladder pain syndrome (IC/BPS), an inflammatory disorder of the bladder of unknown etiology that is more common in those over 50 years old[7, 11, 20, 60]. In a mouse model of IC/BPS, ectopic expression of TNFα in the bladder resulted in heighted pain sensitivity in response to bladder filling[61], but bTLT-like structures were not reported. These results could be due to factors such as age or sex and suggests that multiple processes are required to support these complex structures. Thus, a fine balance of protective inflammatory responses during acute insults and effective resolution of inflammation throughout life may be key to healthy aging. Considering our findings and the role of TNFα in inflamm-aging and bladder disease, clinical studies examining the relationship between age, TNFα levels, and bladder inflammation could provide further insight into these relationships.

While many questions about bTLT remain a mystery, this new finding demonstrates that aging leads to fundamental changes to the bladder characterized by a dramatically different immune landscape. Future work on the aging bladder should consider the presence of bTLT, as they underlie significant changes that likely impact multiple physiologic and homeostatic processes in the bladder. Finally, our single-cell transcriptomic map of bladder immune cells provides a new resource for studying the complexity of the bladder immune system.

Materials and Methods

Mice

All experimental procedures were approved by the animal studies committee of Washington University in St. Louis School of Medicine (Animal Welfare Assurance #A-3381–01) and McMaster University's Animal Research Ethics Board. 2- to 24-month-old C57BL6/J mice were obtained from the National Institute of Aging (NIA). NIA mice are bred and housed 5 mice/cage with wood shavings at Charles Rivers Laboratory on a 12 hr light-dark cycle, at 67–73 deg F and 35–55% humidity, fed sterilized NIH31 food, and provided with water at pH7–7.5 with 4–6 ppm chlorine (see https://www.nia.nih.gov/research/dab/aged-rodent-colonies-handbook/barrier-environmental-information for more information). Upon receipt at Washington University, mice are housed at 5 mice/cage with autoclaved Bed-O'Cobs ¼" (Andersons Lab Bedding) on a 12 hr light-dark cycle, at 68–74 deg F, 30–70% humidity, fed

sterilized Purina Lab Diet 5053, and provided with sterilized tap water. At McMaster University, mice are housed at 5 mice/cage with Teklad 7090 sani-chips on a 12 hr light-dark cycle, at 21–23 deg C, 30–55% humidity, fed Teklad Irradiated Global 14% protein maintenance diet, and provided with sterilized water and an exercise wheel. Germfree (GF) mice were housed at McMaster University Farncombe Family Axenic-Gnotobiotic Facility otherwise in the same conditions except fed Teklad S-2335 diet. Mice were maintained under specified pathogen-free conditions and monitored for mouse pathogens by on-going sentinel testing. *Tnf*$^{-/-}$ (originally from Jackson Laboratories #005540[62]), WT mice (originally from Jackson Laboratories #000664), and GF mice were bred and aged to 18–24 months in house at McMaster University[39]. To account for colony differences, *Tnf*$^{-/-}$ mice and GF mice were compared to age-matched WT mice raised in the same facility. In all studies, mice from multiple cages, cohorts, and facilities (for data with WT only) were analyzed.

Histological and Immunofluorescence analysis

Bladders were aseptically removed, cut in half, and fixed in 10% neutral buffered formalin or methacarn (60% methanol, 30% chloroform, 10% acetic acid), embedded in paraffin, stained with hematoxylin and eosin (7211, Richard-Allen Scientific) and imaged on a Nanozoomer 2.0-HT system (Hamamatsu). Posterior bladder halves were compared within groups. Number and area of bTLTs were determined in 5 sections spaced 150 μm apart using NDP,view2 software (Hamamatsu). Compact aggregates >10,000 μm^2 were considered bTLTs. For immunofluorescence analysis, anterior bladders halves were embedded in OCT Compound (4583, Tissue-Tek) and flash frozen. 7 μm sections were fixed with 1:1 methanol-acetone, rehydrated in PBS, and blocked with Avidin/Biotin Blocking Kit (SP2001, Vector Laboratories) followed by 1% BSA in PBS. Primary antibodies against B220 (13–0452, eBioscience), CD3 (14–0031-82, eBioscience) PNAd (120803, BioLegend), CD31 (ab28364, Abcam), CD138 (142511, BioLegend), CD35 (558768, BD Biosciences), GL7 (13–5902-81, eBioscience), IgA (1040–31, Southern Biotech), and IgD (1120–01, Southern Biotech) were incubated overnight at 4° and detected with streptavidin-conjugated and species-specific secondary antibodies followed by Hoechst dye. Slides were covered slipped with Prolong Gold antifade (P36930, Invitrogen) and imaged on Zeiss Axio Imager M2 microscope with Hamamatsu Flash4.0 camera using Zeiss Zen Pro software.

Organ culture and IgA ELISA

Bladders were aseptically removed, bisected, rinsed with PBS, and both halves cultured together in 500 μL RPMI-1640 with 10% FBS, 1% Pen/Strep (15–140-122, Gibco), 10 mM HEPES, and 1% Glutamax (35030–061, Gibco). Supernatants were removed after 24 hrs and cleared of debris by centrifugation. IgA concentration in urines and culture media was determined by ELISA according to manufacturer protocol (88–50450-22, Invitrogen).

Flow cytometry

Bladders were aseptically removed, minced with scissors, and digested at 37° for 30 minutes in RPMI-1640 with 10mM HEPES, collagenase D (C5318, Sigma-Aldrich), and DNAse (10104159001, Sigma-Aldrich). Bladders were forced through a 70 μm cell strainer (352350, Corning) and washed with 5% FBS in PBS. Single cell suspensions were stained

with anti-CD45-eFluor450 (48–0451-82, eBioscience), anti-CD3-APC (17–0032-82, eBioscience), anti-CD19-PE (115511, BioLegend), anti-CD4-FITC (100405, BioLegend), anti-CD8-PE/Cy7 (100721, BioLegend), anti-CD138-BrillantViolet605 (142515, BioLegend), and 7-AAD (420404, BioLegend). Data was acquired on LSR II flow cytometer (BD) and analyzed with FlowJo software v10.0. Gates were determined with isotype antibodies in bladder suspensions from young mice.

Tissue RNA-sequencing

RNA was purified from snap frozen, homogenized bladders with RNeasy Mini Kit (74101, Qiagen) and RNase-free DNase digestion kit (79254, Qiagen). Libraries were prepared with Ribo-Zero rRNA depletion kit (Illumina) and sequenced on a HiSeq3000 (Illumina). Reads were aligned to the Ensembl GRCm38.76 top-level assembly with STAR version 2.0.4b and gene counts were derived from the number of uniquely aligned unambiguous reads by Subread:featureCount version 1.4.5. Sequencing performance was then assessed for total number of aligned reads, total number of uniquely aligned reads, genes detected, ribosomal fraction, known junction saturation, and read distribution over known gene models with RSeQC version 2.3. All gene counts were then imported into the R/Bioconductor package EdgeR and TMM normalization size factors were calculated to adjust samples for differences in library size. Ribosomal features as well as any feature not expressed in at least 3 samples were excluded from further analysis, and TMM size factors were recalculated to create effective TMM size factors. The TMM size factors and the matrix of counts were then imported into the R/Bioconductor package Limma and weighted likelihoods based on the observed mean-variance relationship of every gene and sample were then calculated with the voomWithQualityWeights function. Generalized linear models were then created to test for gene level differential expression, and differentially expressed genes were then filtered for Benjamini-Hochberg False Discovery Rate (FDR)-adjusted p-values less than or equal to 0.05 and absolute $\log_2$ fold-change ≥1. The $\log_2$ fold-changes for all genes were then imported into the R/Bioconductor packages GAGE and Pathview to find pathways whose mean expression were perturbed versus background with Benajamini-Hochberg FDR-adjusted p-values ≤0.05.

scRNA-seq and cell type identification

Bladders were digested with Multi-tissue dissociation kit (130–110-201, Miltenyi) for 30 min at 37 deg. Bladder cells were filtered, washed, and incubated with magnetic CD45 microbeads (130–052-301, Miltenyi) and purified by 2 sequential positive selections (Fig. S4A). Cells were washed and resuspended at appropriate concentrations for loading into 10X Chromium Controller using the Chromium Single Cell 5’ Library and Gel Bead Kit. Viability was determined by Trypan Blue with a hemocytometer. Reads were processed using cellranger v3.0.1. Filtered outputs were imported into the R package *Seurat* and combined. Default *Seurat* parameters were used unless otherwise noted. Strict filters of >200 genes/cell, <5% mitochondrial reads/cell, <7500 features/cell, and <2500 genes/cell were used. RunPCA was performed on the top 3000 variable genes from FindVariableFeatures. FindNeighbors and FindClusters were used with the first 40 principle components (PCs) and visualized using Uniform Manifold Approximation and Projection (UMAP) (Fig. S2B). Three clusters drove variation attributed to PC1 (Fig. S2C). Expression of urothelial specific

gene *Upk3a* identified urothelial cells in 2 of these clusters; expression of *Dcn* identified stromal cells as the other cluster; and CD45 (*Ptprc*) expression identified the remaining cells as immune cells (Fig. S2D). Urothelial and stromal cells were excluded from further analysis. PCA was again performed on the top 3000 variable genes of this subset. The first 2 PCs demonstrated balanced grouping of approximately 3 main groups of cell types (Fig. S2C). Find Neighbors and FindClusters were used with the first 30 PCs of this subset, resulting in 21 cell clusters. FindAllMarkers was used with min.pct=0.25 to identify cluster-specific genes (Supplemental Table 2). Cell identities were determined by expression of canonical gene markers (Table 1 and Fig. S3). The remaining cell types were identified by literature searches of top differentially expressed genes (Supplementary Table 2) and by loading all cluster markers into the Cluster Identity PRedictor (CIPR)[25] (Supplemental Table 3) web tool (https://aekiz.shinyapps.io/CIPR/). The dot product method was used with ImmGen as the reference database.

RT-qPCR

Bladders were flash frozen or stabilized in RNA Save (01–891-1A, Biological Industries) and RNA extracted using TRIzol reagent (15596018, Invitrogen) according to manufacturer protocol followed by gDNA digestion with TURBO DNA-free kit (AM1907, Invitrogen). cDNA was generated using Superscript II Reverse Transcriptase (18064014, Invitrogen). qPCR was performed with SsoAdvanced Universal SYBR Green Supermix (1725275, Bio-Rad) on a CFX96 Touch Real-Time PCR Detection System (Bio-Rad). Fold-changes were calculated using Ct method and normalized internally to 18S expression.

Statistical analyses

Statistical tests were performed in GraphPad Prism 8. Data sets were evaluated for normality and lognormality with Anderson-Darling, D'Agostino-Pearson, Shipiro-Wilk, and Kolmogorov-Smirno tests. Lognormal distributions were log-transformed and analyzed as a parametric distribution. Unpaired t-tests (with Welch's correction where appropriate) or two-way ANOVA with Bonferroni post-tests were used for parametric data, and Mann-Whitney U test or Kruskal-Wallis with Dunn's multiple comparison tests were used for non-parametric data. $P<0.05$ was considered significant. Data points represent individual animals. Lines represent the mean for normal distributions, geometric mean for log-normal distributions, or median for non-parametric distributions. Error bars represent SEM. For RNA-seq experiments, Benjamini-Hochberg False Discovery Rate (FDR)-adjusted p-values ≤0.05 were considered significant.

Supplementary Material

Refer to Web version on PubMed Central for supplementary material.

Acknowledgments

We thank Drs. Deborah Frank, Jason Mills, and Paula Saz-Leal for editorial comments, the Genome Technology Access Center (GTAC) for performing and processing sequencing data, and Eric Tycksen for bioinformatic analysis and statistical explanations of tissue RNA-seq data.

Funding

This work was funded in part by NIH grants R01 AG052494, P20 DK119840, and R56 AG064634 to IUM; T32 GM007200 and T32 AI007172 to MML; CIHR #153414 to DMEB; Deutsche Forschungsgemeinschaft fellowship #SCHU3131/1–1 to CS; Ontario Early Researchers award to END; NIH Shared Instrumentation Grant S10 RR0275523 to Alafi Neuroimmaging Core; and P30 CA91842 and UL1 TR002345 to GTAC.

REFERENCES

1. Franceschi C, Campisi J. Chronic inflammation (inflammaging) and its potential contribution to age-associated diseases. J Gerontol A Biol Sci Med Sci 2014; 69 Suppl 1: S4–9. [PubMed: 24833586]
2. Niccoli T, Partridge L. Ageing as a risk factor for disease. Curr Biol 2012; 22(17): R741–752. [PubMed: 22975005]
3. McHugh D, Gil J. Senescence and aging: Causes, consequences, and therapeutic avenues. J Cell Biol 2018; 217(1): 65–77. [PubMed: 29114066]
4. Abraham SN, Miao Y. The nature of immune responses to urinary tract infections. Nature reviews Immunology 2015; 15(10): 655–663.
5. Wu XR, Kong XP, Pellicer A, Kreibich G, Sun TT. Uroplakins in urothelial biology, function, and disease. Kidney Int 2009; 75(11): 1153–1165. [PubMed: 19340092]
6. Nygaard I, Barber MD, Burgio KL, Kenton K, Meikle S, Schaffer J et al. Prevalence of symptomatic pelvic floor disorders in US women. JAMA 2008; 300(11): 1311–1316. [PubMed: 18799443]
7. Koziol JA, Adams HP, Frutos A. Discrimination between the ulcerous and the nonulcerous forms of interstitial cystitis by noninvasive findings. The Journal of urology 1996; 155(1): 87–90. [PubMed: 7490906]
8. Suskind AM, Saigal CS, Hanley JM, Lai J, Setodji CM, Clemens JQ et al. Incidence and Management of Uncomplicated Recurrent Urinary Tract Infections in a National Sample of Women in the United States. Urology 2016; 90: 50–55. [PubMed: 26825489]
9. Maserejian NN, Chen S, Chiu GR, Wager CG, Kupelian V, Araujo AB et al. Incidence of lower urinary tract symptoms in a population-based study of men and women. Urology 2013; 82(3): 560–564. [PubMed: 23876577]
10. Ma E, Vetter J, Bliss L, Lai HH, Mysorekar IU, Jain S. A multiplexed analysis approach identifies new association of inflammatory proteins in patients with overactive bladder. Am J Physiol Renal Physiol 2016; 311(1): F28–34. [PubMed: 27029431]
11. Grundy L, Caldwell A, Brierley SM. Mechanisms Underlying Overactive Bladder and Interstitial Cystitis/Painful Bladder Syndrome. Front Neurosci 2018; 12: 931. [PubMed: 30618560]
12. Tyagi P, Tyagi V, Qu X, Lin HT, Kuo HC, Chuang YC et al. Association of inflammaging (inflammation + aging) with higher prevalence of OAB in elderly population. Int Urol Nephrol 2014; 46(5): 871–877. [PubMed: 24323058]
13. Mora-Bau G, Platt AM, van Rooijen N, Randolph GJ, Albert ML, Ingersoll MA. Macrophages Subvert Adaptive Immunity to Urinary Tract Infection. PLoS pathogens 2015; 11(7): e1005044. [PubMed: 26182347]
14. Schiwon M, Weisheit C, Franken L, Gutweiler S, Dixit A, Meyer-Schwesinger C et al. Crosstalk between sentinel and helper macrophages permits neutrophil migration into infected uroepithelium. Cell 2014; 156(3): 456–468. [PubMed: 24485454]
15. Pitzalis C, Jones GW, Bombardieri M, Jones SA. Ectopic lymphoid-like structures in infection, cancer and autoimmunity. Nature reviews Immunology 2014; 14(7): 447–462.
16. Aloisi F, Pujol-Borrell R. Lymphoid neogenesis in chronic inflammatory diseases. Nature reviews Immunology 2006; 6(3): 205–217.
17. Chen SC, Vassileva G, Kinsley D, Holzmann S, Manfra D, Wiekowski MT et al. Ectopic expression of the murine chemokines CCL21a and CCL21b induces the formation of lymph node-like structures in pancreas, but not skin, of transgenic mice. Journal of immunology 2002; 168(3): 1001–1008.
18. Hannan TJ, Mysorekar IU, Hung CS, Isaacson-Schmid ML, Hultgren SJ. Early severe inflammatory responses to uropathogenic E. coli predispose to chronic and recurrent urinary tract infection. PLoS pathogens 2010; 6(8): e1001042. [PubMed: 20811584]

19. Koti M, Xu AS, Ren KYM, Visram K, Ren R, Berman DM et al. Tertiary Lymphoid Structures Associate with Tumour Stage in Urothelial Bladder Cancer. Bladder Cancer 2017; 3(4): 259–267. [PubMed: 29152550]
20. Maeda D, Akiyama Y, Morikawa T, Kunita A, Ota Y, Katoh H et al. Hunner-Type (Classic) Interstitial Cystitis: A Distinct Inflammatory Disorder Characterized by Pancystitis, with Frequent Expansion of Clonal B-Cells and Epithelial Denudation. PloS one 2015; 10(11): e0143316. [PubMed: 26587589]
21. Ellsworth P, Marschall-Kehrel D, King S, Lukacz E. Bladder health across the life course. Int J Clin Pract 2013; 67(5): 397–406. [PubMed: 23574100]
22. Ingersoll MA, Albert ML. From infection to immunotherapy: host immune responses to bacteria at the bladder mucosa. Mucosal Immunol 2013; 6(6): 1041–1053. [PubMed: 24064671]
23. Bruunsgaard H, Andersen-Ranberg K, Hjelmborg J, Pedersen BK, Jeune B. Elevated levels of tumor necrosis factor alpha and mortality in centenarians. Am J Med 2003; 115(4): 278–283. [PubMed: 12967692]
24. Giovannini S, Onder G, Liperoti R, Russo A, Carter C, Capoluongo E et al. Interleukin-6, C-reactive protein, and tumor necrosis factor-alpha as predictors of mortality in frail, community-living elderly individuals. J Am Geriatr Soc 2011; 59(9): 1679–1685. [PubMed: 21883115]
25. Ekiz HA, Huffaker TB, Grossmann AH, Stephens WZ, Williams MA, Round JL et al. MicroRNA-155 coordinates the immunological landscape within murine melanoma and correlates with immunity in human cancers. JCI Insight 2019; 4(6).
26. Heng TS, Painter MW, Immunological Genome Project C. The Immunological Genome Project: networks of gene expression in immune cells. Nature immunology 2008; 9(10): 1091–1094. [PubMed: 18800157]
27. Sivick KE, Schaller MA, Smith SN, Mobley HL. The innate immune response to uropathogenic Escherichia coli involves IL-17A in a murine model of urinary tract infection. Journal of immunology 2010; 184(4): 2065–2075.
28. Liu W, Evanoff DP, Chen X, Luo Y. Urinary bladder epithelium antigen induces CD8+ T cell tolerance, activation, and autoimmune response. Journal of immunology 2007; 178(1): 539–546.
29. Rousseau M, Goh HMS, Holec S, Albert ML, Williams RB, Ingersoll MA et al. Bladder catheterization increases susceptibility to infection that can be prevented by prophylactic antibiotic treatment. JCI Insight 2016; 1(15): e88178. [PubMed: 27699248]
30. Chan CY, St John AL, Abraham SN. Mast cell interleukin-10 drives localized tolerance in chronic bladder infection. Immunity 2013; 38(2): 349–359. [PubMed: 23415912]
31. Trivedi N, Weisel F, Smita S, Joachim S, Kader M, Radhakrishnan A et al. Liver Is a Generative Site for the B Cell Response to Ehrlichia muris. Immunity 2019.
32. Sullivan RT, Kim CC, Fontana MF, Feeney ME, Jagannathan P, Boyle MJ et al. FCRL5 Delineates Functionally Impaired Memory B Cells Associated with Plasmodium falciparum Exposure. PLoS pathogens 2015; 11(5): e1004894. [PubMed: 25993340]
33. Klein RD, Van Pelt CS, Sabichi AL, Dela Cerda J, Fischer SM, Furstenberger G et al. Transitional cell hyperplasia and carcinomas in urinary bladders of transgenic mice with keratin 5 promoter-driven cyclooxygenase-2 overexpression. Cancer Res 2005; 65(5): 1808–1813. [PubMed: 15753378]
34. Jones GW, Jones SA. Ectopic lymphoid follicles: inducible centres for generating antigen-specific immune responses within tissues. Immunology 2016; 147(2): 141–151. [PubMed: 26551738]
35. Mesin L, Ersching J, Victora GD. Germinal Center B Cell Dynamics. Immunity 2016; 45(3): 471–482. [PubMed: 27653600]
36. Uhlen M, Fagerberg L, Hallstrom BM, Lindskog C, Oksvold P, Mardinoglu A et al. Proteomics. Tissue-based map of the human proteome. Science 2015; 347(6220): 1260419. [PubMed: 25613900]
37. Floege J, Boddeker M, Stolte H, Koch KM. Urinary IgA, secretory IgA and secretory component in women with recurrent urinary tract infections. Nephron 1990; 56(1): 50–55. [PubMed: 2234249]

38. Yanagihara T, Kumagai Y, Norose Y, Moro I, Nanno M, Murakami M et al. Age-dependent decrease of polymeric Ig receptor expression and IgA elevation in ddY mice: a possible cause of IgA nephropathy. Lab Invest 2004; 84(1): 63–70. [PubMed: 14631385]
39. Thevaranjan N, Puchta A, Schulz C, Naidoo A, Szamosi JC, Verschoor CP et al. Age-Associated Microbial Dysbiosis Promotes Intestinal Permeability, Systemic Inflammation, and Macrophage Dysfunction. Cell host & microbe 2017; 21(4): 455–466 e454. [PubMed: 28407483]
40. Pabst O, Herbrand H, Friedrichsen M, Velaga S, Dorsch M, Berhardt G et al. Adaptation of solitary intestinal lymphoid tissue in response to microbiota and chemokine receptor CCR7 signaling. Journal of immunology 2006; 177(10): 6824–6832.
41. Claesson MJ, Jeffery IB, Conde S, Power SE, O'Connor EM, Cusack S et al. Gut microbiota composition correlates with diet and health in the elderly. Nature 2012; 488(7410): 178–184. [PubMed: 22797518]
42. O'Brien VP, Hannan TJ, Yu L, Livny J, Roberson ED, Schwartz DJ et al. A mucosal imprint left by prior Escherichia coli bladder infection sensitizes to recurrent disease. Nat Microbiol 2016; 2: 16196. [PubMed: 27798558]
43. Yu Z, Liao J, Chen Y, Zou C, Zhang H, Cheng J et al. Single-Cell Transcriptomic Map of the Human and Mouse Bladders. J Am Soc Nephrol 2019; 30(11): 2159–2176. [PubMed: 31462402]
44. Han X, Wang R, Zhou Y, Fei L, Sun H, Lai S et al. Mapping the Mouse Cell Atlas by Microwell-Seq. Cell 2018; 173(5): 1307. [PubMed: 29775597]
45. Tabula Muris C, Overall c, Logistical c, Organ c, processing, Library p et al. Single-cell transcriptomics of 20 mouse organs creates a Tabula Muris. Nature 2018; 562(7727): 367–372. [PubMed: 30283141]
46. Ovadya Y, Landsberger T, Leins H, Vadai E, Gal H, Biran A et al. Impaired immune surveillance accelerates accumulation of senescent cells and aging. Nat Commun 2018; 9(1): 5435. [PubMed: 30575733]
47. Riley RL, Khomtchouk K, Blomberg BB. Age-associated B cells (ABC) inhibit B lymphopoiesis and alter antibody repertoires in old age. Cell Immunol 2017; 321: 61–67. [PubMed: 28535870]
48. John-Schuster G, Gunter S, Hager K, Conlon TM, Eickelberg O, Yildirim AO. Inflammaging increases susceptibility to cigarette smoke-induced COPD. Oncotarget 2016; 7(21): 30068–30083. [PubMed: 26284585]
49. McDonald KG, Leach MR, Huang C, Wang C, Newberry RD. Aging impacts isolated lymphoid follicle development and function. Immun Ageing 2011; 8(1): 1. [PubMed: 21214915]
50. Hamada H, Hiroi T, Nishiyama Y, Takahashi H, Masunaga Y, Hachimura S et al. Identification of multiple isolated lymphoid follicles on the antimesenteric wall of the mouse small intestine. Journal of immunology 2002; 168(1): 57–64.
51. Sterlin D, Fadlallah J, Slack E, Gorochov G. The antibody/microbiota interface in health and disease. Mucosal Immunol 2020; 13(1): 3–11. [PubMed: 31413347]
52. Sato Y, Mii A, Hamazaki Y, Fujita H, Nakata H, Masuda K et al. Heterogeneous fibroblasts underlie age-dependent tertiary lymphoid tissues in the kidney. JCI Insight 2016; 1(11): e87680. [PubMed: 27699223]
53. Singh P, Coskun ZZ, Goode C, Dean A, Thompson-Snipes L, Darlington G. Lymphoid neogenesis and immune infiltration in aged liver. Hepatology 2008; 47(5): 1680–1690. [PubMed: 18395842]
54. Radl J, Sepers JM, Skvaril F, Morell A, Hijmans W. Immunoglobulin patterns in humans over 95 years of age. Clin Exp Immunol 1975; 22(1): 84–90. [PubMed: 1212818]
55. Tietz NW, Shuey DF, Wekstein DR. Laboratory values in fit aging individuals--sexagenarians through centenarians. Clin Chem 1992; 38(6): 1167–1185. [PubMed: 1596990]
56. Bakun M, Senatorski G, Rubel T, Lukasik A, Zielenkiewicz P, Dadlez M et al. Urine proteomes of healthy aging humans reveal extracellular matrix (ECM) alterations and immune system dysfunction. Age (Dordr) 2014; 36(1): 299–311. [PubMed: 23917802]
57. Thoreux K, Owen RL, Schmucker DL. Intestinal lymphocyte number, migration and antibody secretion in young and old rats. Immunology 2000; 101(1): 161–167. [PubMed: 11012768]
58. James-Ellison MY, Roberts R, Verrier-Jones K, Williams JD, Topley N. Mucosal immunity in the urinary tract: changes in sIgA, FSC and total IgA with age and in urinary tract infection. Clin Nephrol 1997; 48(2): 69–78. [PubMed: 9285142]

59. Yu L, O'Brien VP, Livny J, Dorsey D, Bandyopadhyay N, Colonna M et al. Mucosal infection rewires TNFa signaling dynamics to skew susceptibility to recurrence. Elife 2019; 8.

60. Simon LJ, Landis JR, Erickson DR, Nyberg LM. The Interstitial Cystitis Data Base Study: concepts and preliminary baseline descriptive statistics. Urology 1997; 49(5A Suppl): 64–75. [PubMed: 9146004]

61. Yang W, Searl TJ, Yaggie R, Schaeffer AJ, Klumpp DJ. A MAPP Network study: overexpression of tumor necrosis factor-alpha in mouse urothelium mimics interstitial cystitis. Am J Physiol Renal Physiol 2018; 315(1): F36–F44. [PubMed: 29465304]

62. Pasparakis M, Alexopoulou L, Episkopou V, Kollias G. Immune and inflammatory responses in TNF alpha-deficient mice: a critical requirement for TNF alpha in the formation of primary B cell follicles, follicular dendritic cell networks and germinal centers, and in the maturation of the humoral immune response. J Exp Med 1996; 184(4): 1397–1411. [PubMed: 8879212]

63. Bando JK, Nussbaum JC, Liang HE, Locksley RM. Type 2 innate lymphoid cells constitutively express arginase-I in the naive and inflamed lung. J Leukoc Biol 2013; 94(5): 877–884. [PubMed: 23924659]

64. Miller JC, Brown BD, Shay T, Gautier EL, Jojic V, Cohain A et al. Deciphering the transcriptional network of the dendritic cell lineage. Nature immunology 2012; 13(9): 888–899. [PubMed: 22797772]

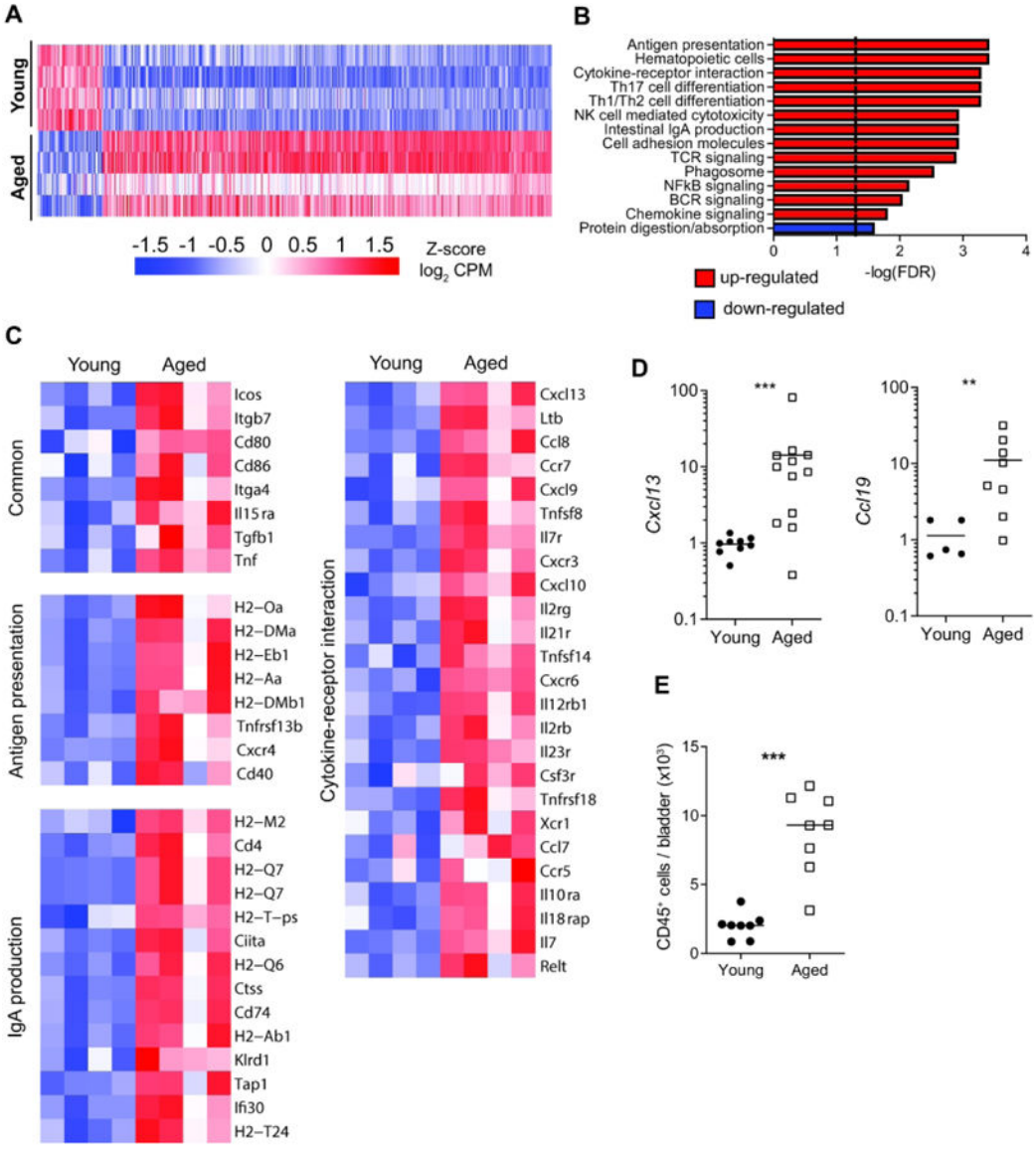

Figure 1. Tissue transcriptomic map of young and aged bladders.

(**A**) Heatmap of the global tissue transcriptome of young and aged bladders with fold change >2 and Benjamini-Hochberg FDR-adjusted P<0.05. n= 4 bladders/group. (**B**) Significantly enriched KEGG pathways based on fold change of all genes. (**C**) Heatmaps of significantly different genes from select significant KEGG pathways. (**D**) Gene expression validation by qRT-PCR in whole bladders (n=5–11/group). (**E**) Number of $CD45^+$ cells/bladders from young and aged mice (n=8/group) determined by flow cytometry. Line at median. ***p<0.001, **p<0.01, Mann-Whitney U-test.

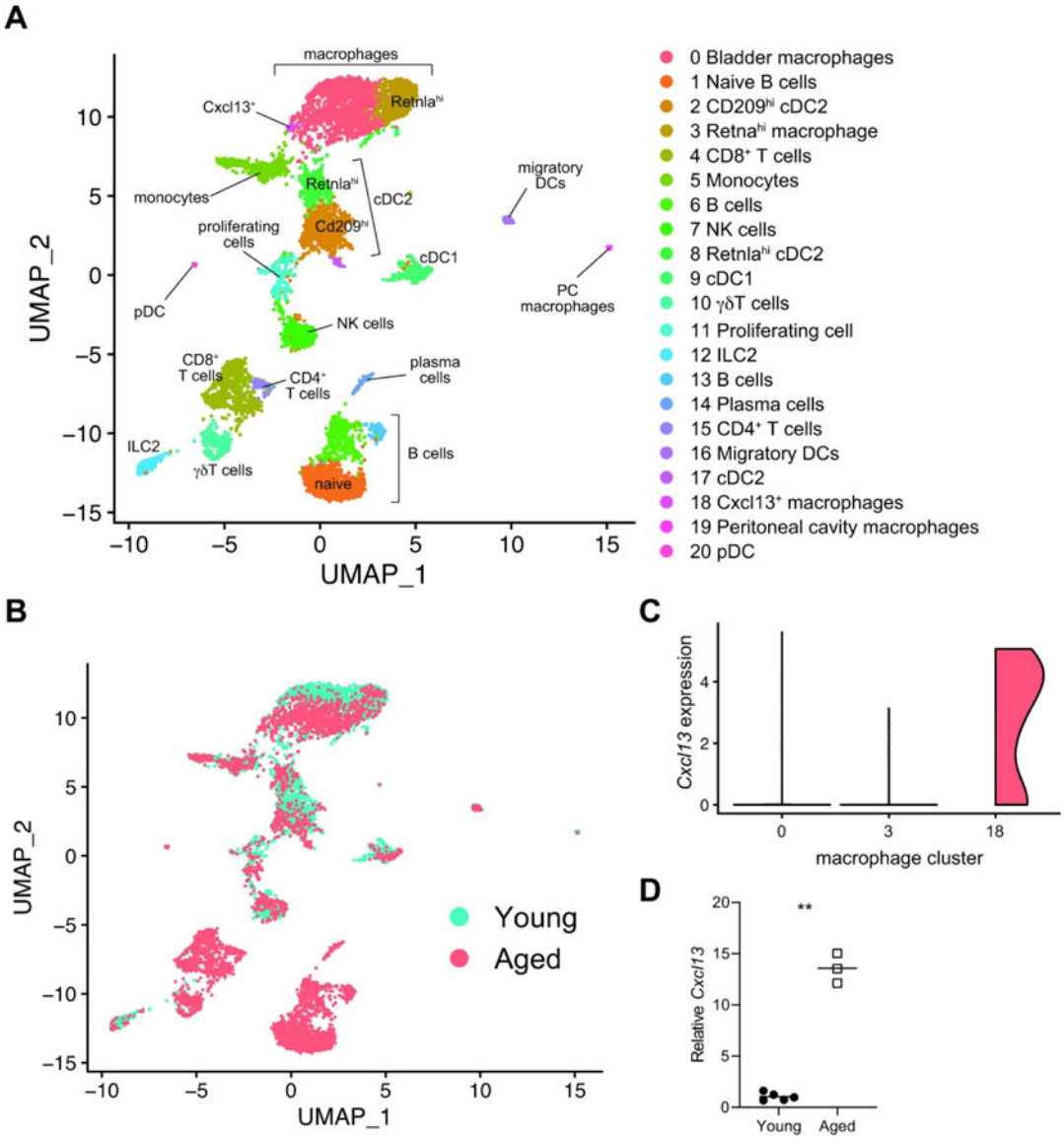

Figure 2. Single cell transcriptomic map of immune cells from young and aged bladders.

(**A**) Clustering analysis and cell type identification of CD45+ cells from young (n= 3209) and aged bladders (n=4682). Cluster numbers are ordered by most abundant cell type from the merged data set. (**B**) Map of cells originating from young or aged bladders. (**C**) Expression of *Cxcl13* in scRNA-seq macrophage clusters (numbered as in A and colored as in B). (**D**) RT-qPCR of sorted F4/80^{+}CD64^{+}Ly6C^{-} macrophages from young and aged mice (n=3–5/group). **p<0.01, Unpaired t-test with Welch's correction. Lines at mean.

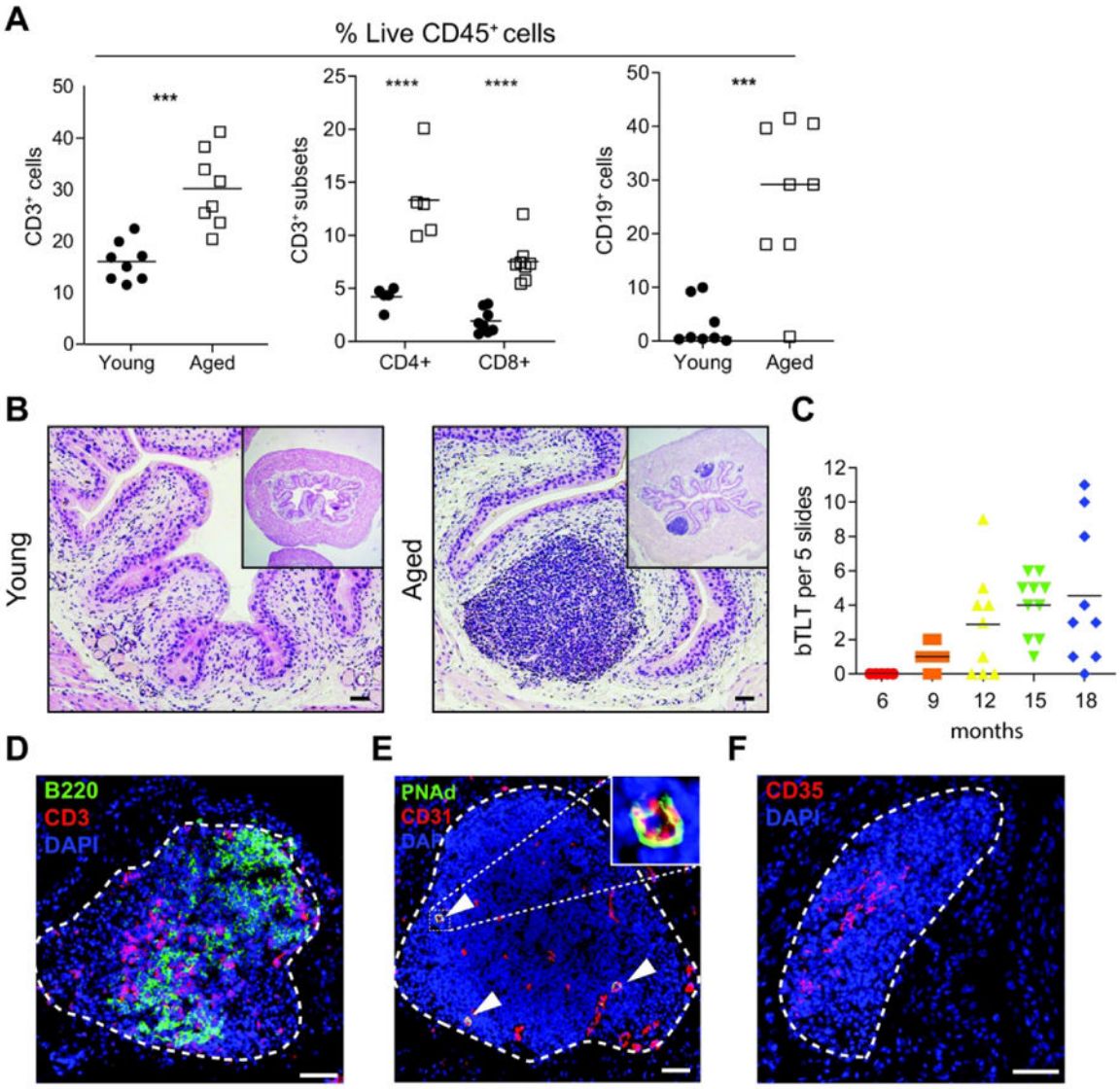

Figure 3. Lymphoid infiltrates form bladder tertiary lymphoid tissues (bTLT) during aging.

(**A**) Frequency of B cells, T cells, and T cell subsets among live CD45^{+} cells in young and aged bladders by flow cytometry. n=5–8 per group. (**B**) Representative H&E images of young and aged bladders. (**C**) Number of bTLT over the life course of mice n=5–10/group. (**C**) Representative image of B cells (B220^{+}, green) and T cells (CD3^{+}, red) in segregated zones within bTLT in aged mice. (**D**) Representative image of CD31^{+}(red) PNAd^{+}(green) high endothelial venules (white arrowheads) within bTLT in aged mice. (**E**) Representative image of CD35^{hi} follicular dendritic cell network within bTLT in aged mice. All nuclei stained with DAPI (blue). All scale bars, 50 μm.

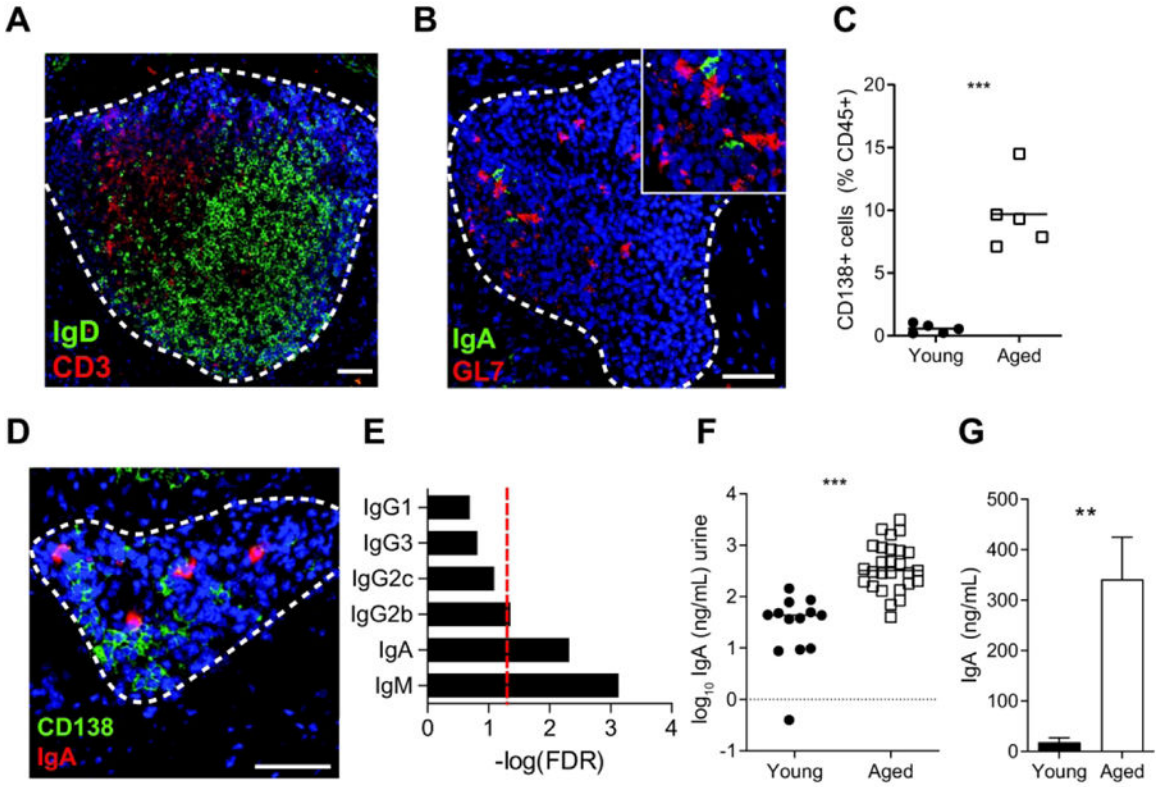

Figure 4. bTLT are centers for B cell recruitment, activation, germinal center reactions, and plasma cell differentiation.

(**A**) Representative image of naive B cells (IgD+, green) and T cells (CD3+, red) within bTLT of aged bladders. (**B**) Representative image of IgA+ cells within a GL7+ (green) germinal center of a bTLT. (**C**) Frequency of live CD45+CD138+ plasma cells in young and aged bladders by flow cytometry. n=5/group. (**D**) Representative image of IgA+CD138+ plasma cells within bTLT of aged bladders. (**E**) FDR -adjusted P values of IgM and class-switched isotypes from tissue RNA-seq of young and aged bladders. Red line, p=0.05. (**F**) Concentration of IgA in urine of young (n=13) and aged (n=27) mice. (**G**) Concentration of IgA in supernatants of young and bladders cultured *ex vivo* for 24 hours. n=5/group. All scale bars, 50 μm. **p<0.01, ***p<0.001. Mann-Whitney U test.

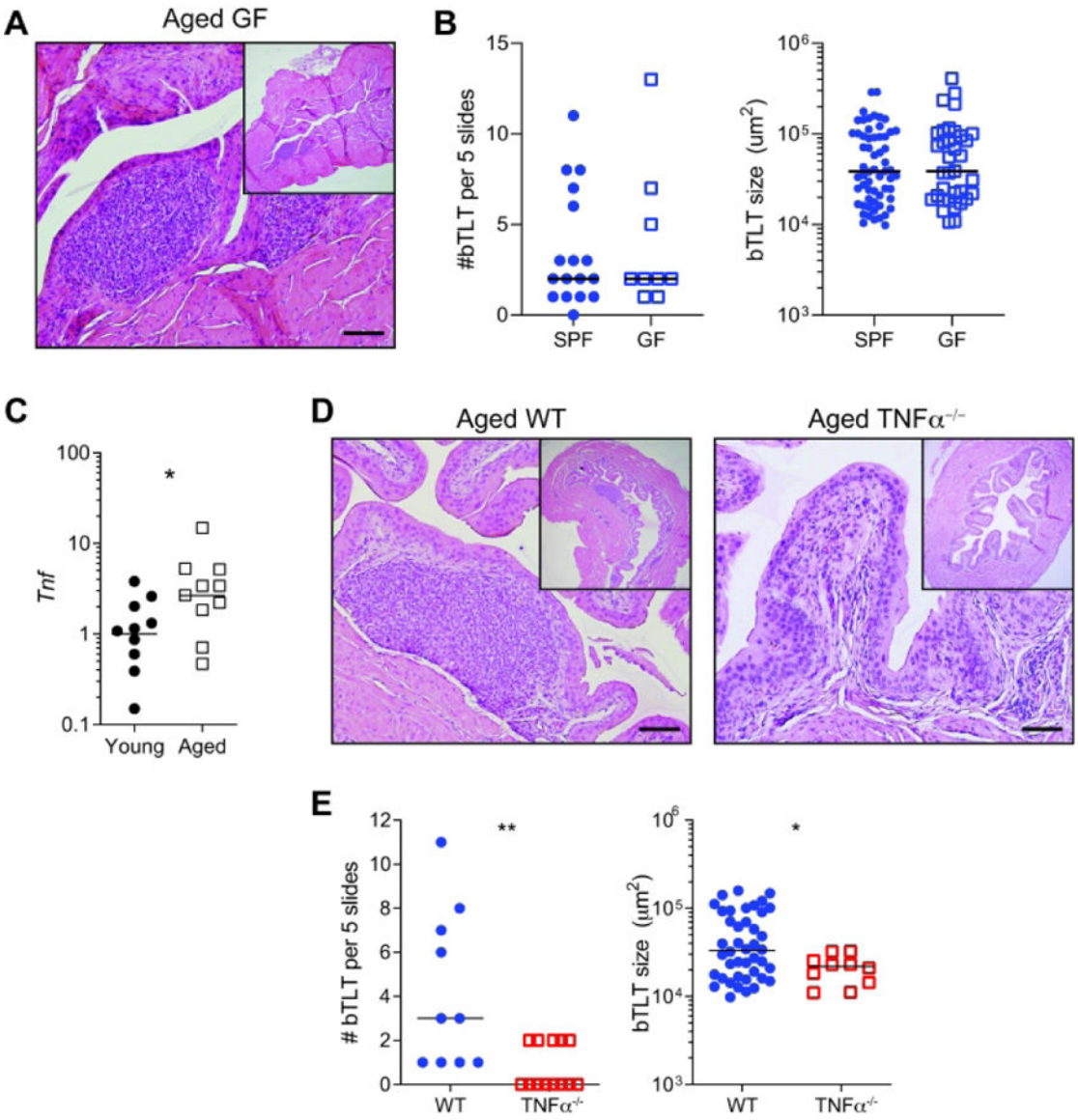

Figure 5. bTLT size and number are independent of microbial status and dependent on age-associated TNFα.

(**A**) Representative H&E image of WT aged germ free (GF) bladders. (B) Number and size of bTLT found in WT specific pathogen free (SPF) and GF bladders. n=9–17/group. (**B**) Relative expression of *Tnf* and in young and aged bladders by RT-qPCR. n=10/group. (**C**) Representative H&E images of aged WT and TNFα$^{-/-}$ bladders. (**C**) Number and size of bTLT in aged WT and TNFα$^{-/-}$ bladders. Lines at median. *p<0.05, **p<0.01, Mann-Whitney U-test. Scale bars, 100 μm

Table 1.

Markers used to identities cell cluster identities from scRNA-seq

Cluster Number/Name	Cell Identity Markers	Top CIPR[25, 26] match
0 - Macrophages	*Adgre1*	Interstitial macrophage (lung)
1 - B cells (naïve)	*Cd79a, Ms4a1, Ighd*	Spleen follicular B cell
2 - cDC2 (CD209)	*Mgl2*	Adipose tissue CD11b− DC
3 - Macrophages (Retnla^{hi})	*Adgre*	Interstitial macrophage (lung)
4 - CD8+ T cells	*Cd3d, Cd3g, Cd3e, CD8b1, Gzmk*	Naïve CD8+ T cell 96 hours after in vitro stimulation
5 - Monocytes	*Ly6c2*	Blood Ly6C+ MHCII+ monocytes
6 - B cells (activated)	*Cd79a, Ms4a1, Ctla4, Mzb1*	Marginal zone B cell
7 - NK cells	*Gzma, Gzmb*	Splenic NK cell Ly49H+ subset
8 - cDC2 (Retnla^{hi})	*Sirpa, Mgl2*	Adipose tissue CD11b+ DC
9 - cDC1	*Flt3, Xcr1, Clec9a*	Adipose tissue CD11b− DC
10 - γδT cells	*Tcrd, Tcrg, Tcre*	Thymus B6 E15 TCRgammadelta
11 - Proliferating cells	*Mki67, Top2a, Ube2c*	Pre-T cell double positive blasts *
12 - ILC2	*Il2ra, Gata3, Arg1*[63]	Innate lymphoid cells type 2 (intestine)
13 - B cells (clonally expanded)	*Cd79a, Ms4a1, Ighv1–58, Igkv6–15*	B cell (marginal zone)
14 - Plasma cells	*Jchain*	Pre-T cell double positive all
15 - CD4+ T cells	*Cd3d, Cd3g, Cd3e, Cd4*	CD4+ T cell 8 days after LCMV infection
16 - Migratory DCs	*Flt3, Fscn1, Cacnb3, Nudt17, Socs2*[64]	Skin draining lymph node DC
17 - cDC2	*Flt3, Sirpa, Mgl2*	Thymus double negative DC
18 - Macrophages (Cxcl13^{+})	*Adgre1*	F4/80hi liver macrophage
19 - Macrophages (peritoneal)	*Adgre1*	Peritoneal macrophage steady state
20 - pDC	*Flt3, Pacsin1, Siglech, Irf8, Cox6a2, Runx2*[64]	Spleen CD8- plasmacytoid DC

* Proliferating cells most closely matched Immgen cell types that are rapidly dividing due to the strong influence of cell cycle genes